Recent progress in reduced-scale modelling of vehicle interior noise

V.V. Krylov, V.B. Georgiev and R. Gorman
Department of Aeronautical and Automotive Engineering,
Loughborough University,
Loughborough, Leicestershire LE11 3TU, UK
e-mail: **V.V.Krylov@lboro.ac.uk**

Abstract
The paper gives a review of the recent research into simplified reduced-scale models of structure-borne vehicle interior noise carried out in Loughborough University. The models under consideration evolve from the simplest ones to more sophisticated developments that take into consideration some important structural dynamic and acoustic features of real vehicles. Analytical and numerical approaches to the theoretical description of such models are discussed. The results of theoretical calculations are compared with the measurements on some reduced-scale models. The comparison of the theory with the measurements demonstrates that simplified reduced-scale models can be used successfully for studying interior noise in real road vehicles. One of the most important issues in this approach is to find a compromise between the minimum degree of complexity of a model and the required accuracy of description of frequency contents and noise levels in a real vehicle.

1 Introduction

Vehicle interior noise can be air-borne or structure-borne. Both these types of noise are characterised by a variety of mechanisms of excitation and interaction of structural vibrations of the car body and of acoustic modes of the interior cavity. A number of different modelling techniques based on finite element calculations or on combined numerical and experimental approaches have been developed to describe vehicle interior noise (see, e.g. [1-5]). Although certain important advances have been made in this field, the theoretical models that are currently available are too time consuming and still not accurate and robust enough to be relied upon by car designers and manufactures. Therefore, further research is needed to improve the understanding of vehicle interior noise.

A promising and efficient approach to modelling and understanding of vehicle interior noise can be based on analytical techniques employing maximum possible simplification of the model vehicle structure and of the acoustic interior [6]. The results of this approach can be expressed in terms of analytical formulae for sound pressure in the vehicle interior as a function of road irregularity, vehicle speed, properties of suspensions, resonance frequencies and modal shapes of structural and acoustical modes and of their coupling to each other.

In addition to analytical modelling, a very helpful approach to understanding and predicting vehicle interior noise can be based on the development of reduced-scale physical models and their subsequent theoretical and experimental investigation. These could provide a researcher with the flexibility to easy change the parameters of the vehicle under development and to measure the influence of these parameters on generated interior noise. Earlier developed reduced-scale models were designed mainly to reflect only acoustic properties of vehicle interiors (see, e.g. [7,8]). In the course of recent investigations with reduced-scale models carried out in Loughborough University [9,10] both structural and acoustic subsystems, as well as their interaction, have been investigated. In the present paper a brief review of these investigations will be given, starting from the simplest model, QUASICAR, and continuing with more complex but still manageable reduced-scale models.

Note in this connection that, if the possibility of scaling of purely acoustic physical models is quite obvious, i.e. the reduction of linear dimensions by N times results in the increase in resonant frequencies by N times, it is not so obvious in the case of structural modes. Indeed, vibration fields in structures are combinations of many different types of elastic waves that can propagate in bounded solids. Some of these waves are dispersive, some are not. Therefore, it is not so easy to tell how the resonant frequencies and modal shapes of structural vibration modes will change with the scaling. For simple structures, such as finite plates, one can prove that if all linear dimensions of a plate, i.e. length, width and height, will be reduced by N times, than the resonance frequencies of the plate will increase by the same number N. One can expect that this is true for arbitrary solid structures as well, which is the necessary prerequisite of reduced-scale structural-acoustic modelling. Note that structural and acoustic attenuations have different laws of frequency dependence for different physical mechanisms of energy loss. Therefore, generally speaking, attenuation can not be scaled. A more detailed discussion of these general aspects of elasto-dynamics is, however, beyond the scope of this paper.

2 Outline of the theory

2.1 Acoustic pressure of structure-borne interior noise

In the case of a concentrated dynamic force applied to a model vehicle body, e.g. from the front-right suspension, the structure-borne acoustic pressure in a vehicle interior can be expressed in the form [6]

$$p'(\mathbf{r}) = \frac{4c^2\rho_0 P_{fr}(\omega)}{\omega^2 \rho_{0s} h_s V} \sum_{m=0}^{\infty} \sum_{p=1}^{\infty} a_m F_{mp}(\omega) S_{mp} \Phi_m(\mathbf{r}) \Psi_p(\boldsymbol{\rho}_{fr}) . \tag{1}$$

Here

$$F_{mp}(\omega) = \frac{\omega^4}{(\omega_m{}^2 - \omega^2 - 2i\delta_m\omega)(\omega_p{}^2 - \omega^2 - 2i\delta_p\omega)} \tag{2}$$

and

$$S_{mp} = \frac{1}{L_l L_y} \int_S \Phi_m(\mathbf{r}') \Psi_p(\boldsymbol{\rho}') d\mathbf{r}' . \tag{3}$$

The notations used in Eqns (1)-(3) are the following: $P_{fr}(\omega)$ is the frequency spectrum of the applied force, c and ρ_0 are sound velocity and mass density of air, h_s, L_y and ρ_{0s} are thickness, width and mass density of the thin-walled structure (e.g. plate or shell) simulating an enclosed vehicle interior, L_l is the total 'unwrapped' length of the above structure, $\Phi_m(\mathbf{r})$, and $\Psi_p(\boldsymbol{\rho})$ are modal shapes of acoustic and structural modes respectively, δ_m and δ_p are their attenuation decrements, and a_m are coefficients depending on the acoustic mode type and on the shape of the enclosure.

The non-dimensional function $F_{mp}(\omega)$ defined by Eqn (2) can be termed as the frequency overlap function of the acoustical and structural modes characterised by the overall modal indexes m and p. Similarly, the non-dimensional factor S_{mp} defined by Eqn (3) can be considered as coefficient of spatial coupling between the corresponding acoustical and structural modes. It is the product $F_{mp}(\omega)S_{mp}$ that determines the amplitudes of the resulting acoustic pressure inside the vehicle compartment. Note that Eqns (1)-(3) have been derived using the assumption of negligibly small effect of air loading on structural vibrations in a car body (for discussion of this approximation see books [11,12]).

For the sake of simplicity, Eqn (1), in contrast to the similar expression in [6], does not consider road irregularity and the corresponding transfer function linking it with the dynamic suspension forces. One can see from Eqn (1) that the resulting acoustic pressure is formed as a summation over products of all structural and acoustic modes. However, because of the double filtration – over time and space described

by the products $F_{mp}(\omega)S_{mp}$ – only relatively few of the structural and acoustical modes interact effectively and give noticeable contributions. First of all, it is clear from Eqn (2) that only those acoustic and structural modes should be taken into account which resonance frequencies, ω_m and ω_p respectively, are close enough to each other. In addition to this, it follows from Eqn (3) that only those overlapping acoustical and structural modes should be taken into account for which the values of the mode coupling coefficients S_{mp} are big enough.

2.2 Analysis of structural modes.

The simplest approximation for structural modes used in [6] considered a car body as a curved simply supported plate with the profile shown on Figure 1, in which any curvature effect on flexural wave propagation have been neglected. Such an approximation is appropriate only for relatively high frequencies, i.e. for frequencies higher than the ring frequency of the circular shell with the radius corresponding to the smallest radius of curvature in the structure. For low and medium frequencies one should consider even very simplified car structures as non-circular cylindrical shells, which means that the effect of local curvature should be considered as significant.

According to finite element analysis of flexural vibrations in the above-mentioned simplified model of vehicle body built up of a non-circular cylindrical shell (this model has been also used for experimental investigations of vehicle interior noise [9,10]), resonant vibration modes of such a structure can be represented as symmetric and anti-symmetric combinations of vibrations of their quasi-flat parts taken separately [13]. It is interesting that at low frequencies the values of resonant frequencies of symmetric and anti-symmetric modes are very close to each other and to resonant frequencies of simply-supported plates with the dimensions equal to the dimensions of the shell's quasi-flat parts.

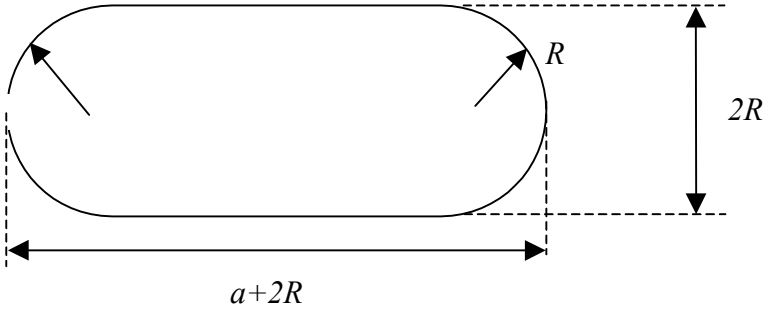

Figure 1: Profile of the non-circular cylindrical shell used for experimental modelling of structure-borne vehicle interior noise [9,10]

The same conclusion can be also drawn using the recently developed analytical approach utilising the concept of coupled-waveguide propagation along quasi-flat areas of shells having the same non-circular shape but an infinite length (depth) [14]. The physical reason for waveguide propagation along quasi-flat parts of non-circular cylindrical shells is the difference between flexural wave velocities in their flat and curved areas. In particular, for waveguide propagation it is necessary that the velocity of flexural waves in the flat area is lower than their velocity in the adjacent circular cylinders. This is always the case for flexural wave propagation in near-axial directions of circular cylindrical shells. One can employ the approximate expressions for flexural wave velocities (or wavenumbers) in circular shells with different radii of curvature to derive the dispersion equations for waves propagating in the waveguides comprising infinitely long flat plates (strips) bounded by fragments of two circular shells. The coupling between two neighbouring waveguides and the coupled waveguide modes in the entire shell should be taken into account on the next stage. After that, considering shells of finite length, the transition can be made from coupled guided modes to coupled resonant vibrations of quasi-flat parts of the shells. It can be

demonstrated that resonant frequencies and spatial distributions of the resultant vibration modes are in good agreement with the experiments [9,10] and with the results of finite element calculations [13].

2.2.1 Coupled-wave theory approach to calculation of structural modes

Let us discuss the coupled-wave theory approach in more detail. As an example, let us consider the waveguide propagation of flexural waves in an infinitely long flat plate (strip) of thickness h and width a bounded by fragments of two cylindrical shells with equal radii R (Figure 2). It is assumed that the shells are of the same thickness h as the flat plate. Such a structure can be considered as a three-layered anisotropic medium for flexural waves, the middle layer (a flat isotropic strip) being characterised by a lower velocity of flexural waves in comparison with flexural wave velocities in the near-axial direction in the adjacent cylindrical shells. It is assumed initially that the above-mentioned structure is infinite in z-direction ($L = \infty$).

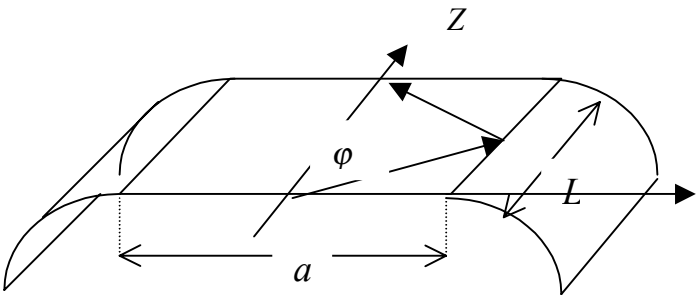

Figure 2. Waveguide propagation of flexural waves in an infinitely long flat plate (strip) bounded by two circular cylindrical shells.

The waveguide propagation in such a structure can be described by the well-known general dispersion equation for three-layered acoustic media that should be modified for the considered case of shell-induced anisotropic side layers:

$$\frac{a}{2}\left[k_{pl}{}^2 - \gamma^2\right]^{1/2} = m\frac{\pi}{2} + \tan^{-1}\left[\frac{\gamma^2 - k_{sh}{}^2(\varphi)}{k_{pl}{}^2 - \gamma^2}\right]^{1/2}. \tag{4}$$

Here γ is yet unknown wavenumber of a guided wave propagating in the above-mentioned three-layered system, $k_{pl} = (\omega^2\rho_s h/D)^{1/4}$ is the wavenumber of flexural waves in a flat plate, where ρ_s is the mass density of the plate material and D is flexural rigidity, $k_{sh}(\varphi)$ is the angular-dependent wavenumber of flexural waves in a circular cylindrical shell, and $m = 0,1,2,3\ldots$ Note that

$$\gamma = k_{pl}\cos\varphi, \tag{5}$$

where φ is the angle of propagation of two plane waves comprising a guided mode (see Figure 2). The guided wave field propagating in the flat plate area is described as

$$w_{pl} = \cos[(k_{pl}{}^2 - \gamma^2)]^{1/2} x]\ \exp(i\gamma z - i\omega t), \tag{6}$$

and the guided wave field penetrating into the adjacent shells is

$$w_{sh} = C \exp\left[-(\gamma^2 - k_{sh}^2(\varphi(\gamma)))^{1/2} |x_{sh}|\right] \exp(i\gamma z - i\omega t). \quad (7)$$

Here x_{sh} is the surface curvilinear coordinate that extends the coordinate x from the plate to the shell area, and C is the constant determined from the continuity condition at the boundaries between the plate and the shells.

To find γ from the dispersion equation (4) one has to use appropriate analytical expressions for the wavenumber of flexural waves in the shell $k_{sh}(\varphi)$ propagating at arbitrary angle φ in respect of the axial direction of the shell. It is well known that propagation of flexural waves in shells is governed by bending and membrane effects, which makes the expressions for flexural wavenumbers rather complex in different practical situations. Their functional appearance depends on the characteristic parameters of the shell, in particular on its ring frequency $\omega_r = c_l'/R$, where c_l' is the velocity of a quasi-longitudinal wave in a thin flat plate (plate wave velocity), and R is radius of the shell's curvature.

Let us consider the most interesting case of waveguide propagation of flexural waves at frequencies lower than the ring frequency. In this case the expressions for $k_{sh}(\varphi)$ are generally too complex to be described analytically [11,12]. For illustration purposes we limit ourselves with the case of small wave propagation angles φ, for which $k_{sh}(\varphi)$ is known to be extremely small. To simplify things even further, we assume that $k_{sh}(\varphi) = 0$ for all φ in the range of interest. In this case the dispersion equation (4) can be rewritten in the form

$$\frac{a}{2}\left[k_{pl}^{\ 2} - \gamma^2\right]^{1/2} = m\frac{\pi}{2} + \tan^{-1}\left[\frac{\gamma^2}{k_{pl}^{\ 2} - \gamma^2}\right]^{1/2}. \quad (8)$$

Keeping in mind that $\cos\varphi = 1 - \varphi^2/2$ for small φ and substituting Eqn. (5) into Eqn. (8), one can derive the following simplified equation versus φ:

$$\frac{a}{2}k_{pl}\varphi = m\frac{\pi}{2} + \tan^{-1}\left[\frac{1-\varphi^2}{\varphi^2}\right]^{1/2}. \quad (9)$$

Noticing that for small φ the last term in the right hand side of Eqn. (9) is approximately equal to $\pi/2$, one can reduce Eqn. (9) to

$$\frac{a}{2}k_{pl}\varphi = (m+1)\frac{\pi}{2}, \quad (10)$$

from which it follows that $\varphi = (m + 1)\pi/ak_{pl}$. Substituting this solution into Eqn. (5), one can derive the following approximate expression for the wavenumbers of guided flexural waves propagating in the above system at frequencies that are below the ring frequency:

$$\gamma = k_{pl}\left[1 - \frac{(m+1)^2\pi^2}{2a^2k_{pl}^{\ 2}}\right]. \quad (11)$$

Note that in the case under consideration the waveguide effect is rather strong, and the energy of a guided wave is almost entirely concentrated in the flat plate area.

Let us now consider a finite value of the length L of the above-mentioned plate/shell system and assume for simplicity that at $z = 0$ and at $z = L$ the system is subject to simply supported boundary conditions.

Then the distribution of the resulting elastic field along z-axis formed by incident and reflected guided waves can be expressed in the form $sin(\gamma z)$. Using the condition $sin(\gamma L) = 0$, one can obtain that $\gamma L = \pi n$, where $n = 1,2,3\ldots$ Applying this to Eqn. (11), one can obtain the following equation for the system's resonant frequencies:

$$\omega_{mn} = \left(\frac{D}{\rho_s h}\right)^{1/2}\left[\frac{\pi^2(m+1)^2}{a^2} + \frac{\pi^2 n^2}{L^2}\right]. \tag{12}$$

Keeping in mind that in the case considered $m = 0,1,2,$, one can notice that Eqn. (12) coincides with the well-known expression for resonant frequencies of simply supported plates having the dimensions L and a. This reflects the fact that at frequencies lower than the ring frequency the waveguide effect created by two adjacent circular shells is very strong and almost the whole vibration energy is concentrated in the flat plate area. One should keep in mind, however, that Eqn. (12) is valid for $n >> m$, which corresponds to low values of the propagation angle φ considered in the above-mentioned approximate solution.

Let us now briefly discuss the effect of coupling between the neighbouring waveguides, which should be taken into account if the entire shell is considered. Not mentioning here the wave-coupling equations (for more detail see [14]), we only note that in the case of low frequencies, i.e. for frequencies lower than the ring frequency of the circular shell associated with curved parts, the wave coupling between the vibration fields in quasi-flat areas is very weak. Therefore, the equation of a single simply-supported plate can be used for calculation of resonant frequencies of both symmetric and anti-symmetric modes of the whole shell. This agrees well with the recent experiments [9,10] and with the finite element calculations [13]. Such calculations show that resonant frequencies of symmetric and anti-symmetric modes of the non-circular cylindrical shells under consideration are practically the same (a small difference appears only in the fifth digit). In the same time, the numerical routine clearly identifies the existence of symmetric and anti-symmetric modes in the calculated distribution of vibrations over the shell cross-section.

Numerically calculated distributions of vibration fields for lowest order symmetric and anti-symmetric modes of the non-circular cylindrical shell made of steel and having two quasi-flat surfaces are shown on Figure 3.

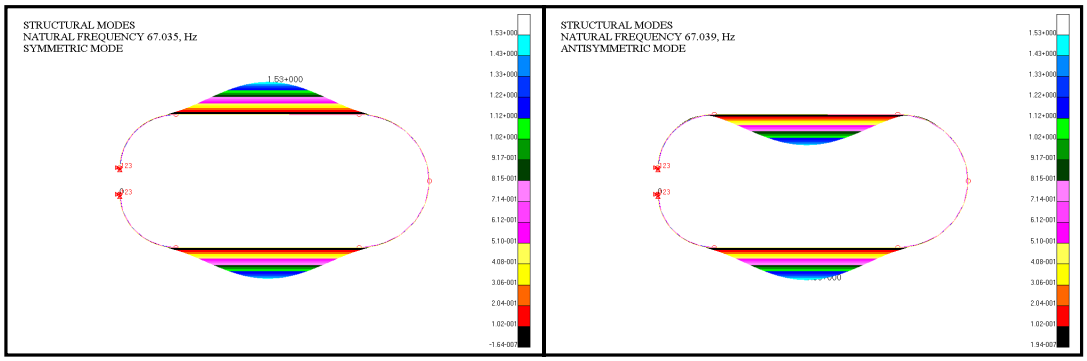

Figure 3: Numerically calculated distributions of vibration fields for lowest order symmetric and anti-symmetric modes of the non-circular cylindrical shell made of steel and having two quasi-flat surfaces [13] (see also Figure 1); geometrical parameters of the shell are: radius R = 125 mm, the total length a + 2R = 550 mm, the width L = 300 mm, and the shell thickness h = 1.2 mm; resonant frequencies of the symmetric and anti-symmetric modes are 67.035 Hz and 67.039 Hz respectively.

Figure 4 illustrates numerically calculated distributions of vibration fields of higher-order symmetric and anti-symmetric modes of the same structure [13].

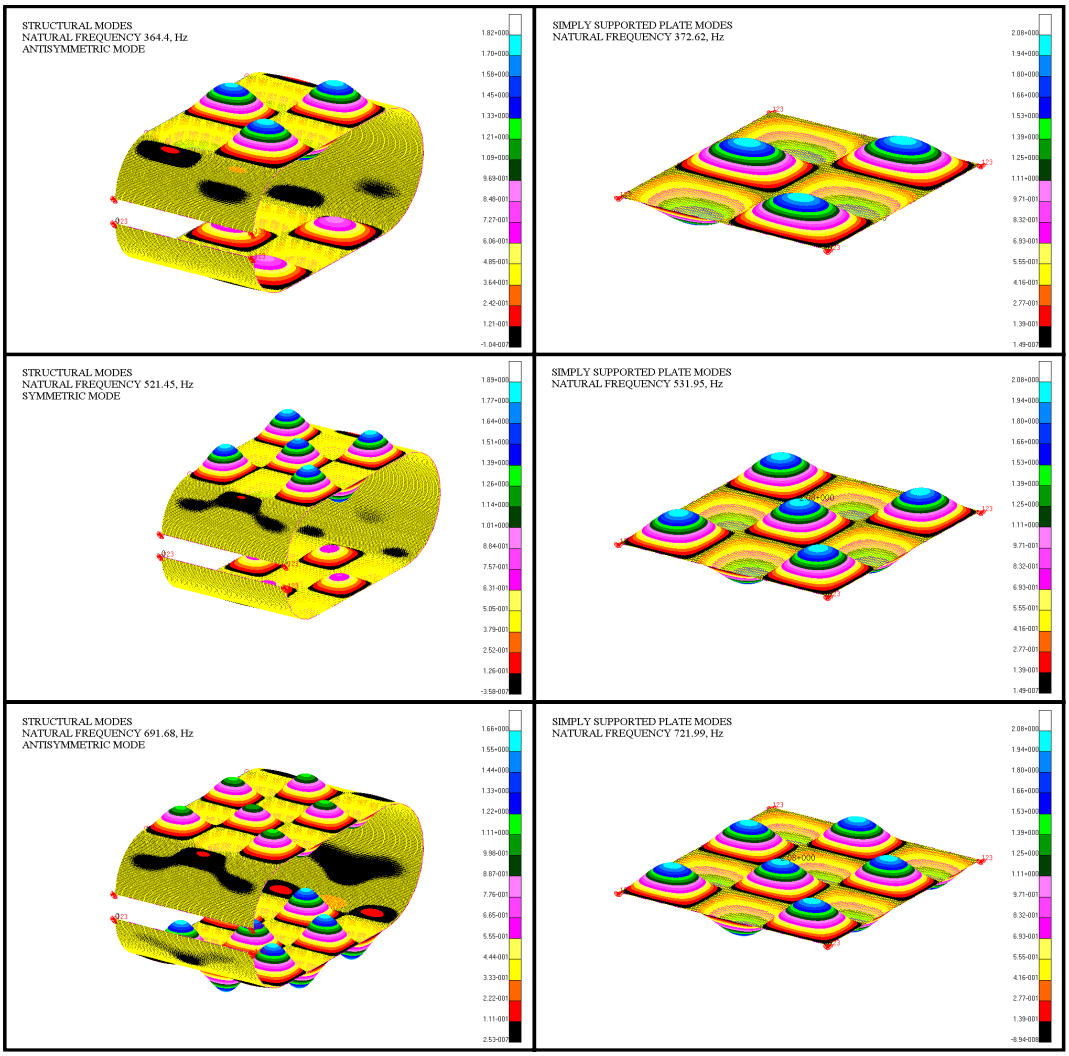

Figure 4: Numerically calculated distributions of vibration fields for higher-order modes of the non-circular cylindrical shell made of steel and having two quasi-flat surfaces (left) and of a rectangular plate with the dimensions of the shell's quasi-flat surfaces (right) [13]; parameters of the shell are the same as in Figure 3.

2.2.2 Structural modes of some modified structures

For more complex models of vehicle structures vibration modes are very difficult to calculate analytically. Therefore, finite element methods remain the only available tool. In particular, some resonant frequencies and modal shapes have been calculated using finite elements for two modified structural models based on the basic model shown on Figure 1 (see [13]). In the first model, model ***M1***, the geometry and the boundary conditions were the same as those shown on Figure 1. The only difference was in the higher thickness of the bottom plate, which was now equal to 6.0 mm. In that way the symmetry in respect of the horizontal plane has been broken, which corresponded more realistically to real road vehicles. Numerically calculated distributions of vibration fields for some structural modes of

the modified model ***M1*** are shown of Figure 5. One can see that at lowest resonant frequency only the roof area is vibrating. At higher frequencies the bottom and curved parts are vibrating as well.

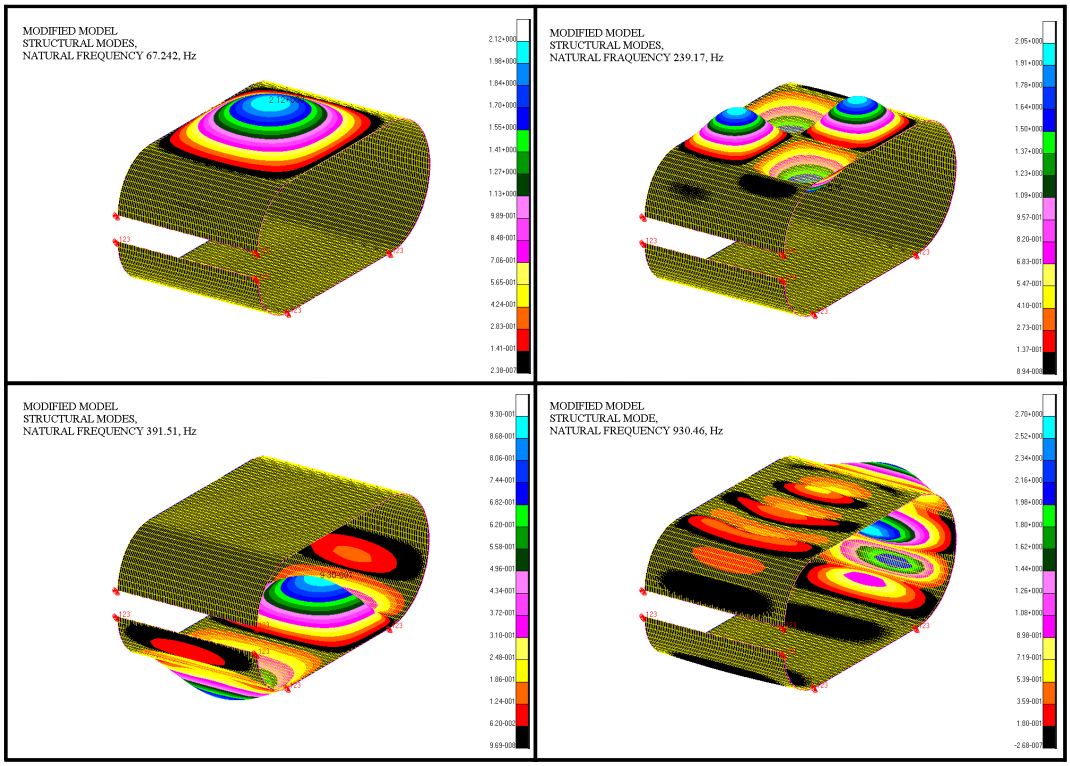

Figure 5: Numerically calculated distributions of vibration fields for some structural modes of the modified model ***M1*** [13].

The second modified model, model ***M2***, incorporated changes in boundary conditions and in the structure of the bottom part (see Figure 6). In particular, the simply supported boundary conditions of the basic model have been replaced by the beams with a circular cross section, and the bottom plate was stiffened by the two beams in transverse and longitudinal directions (for more detail see [13]).

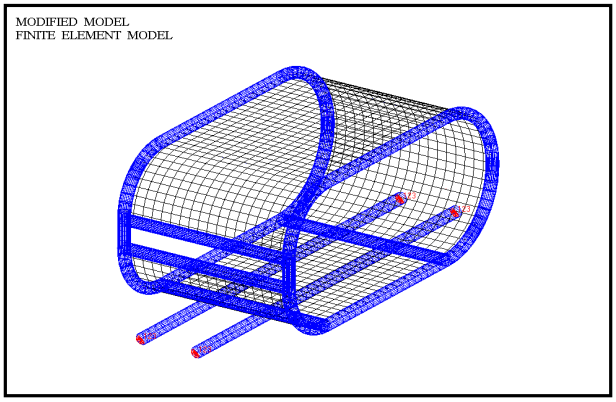

Figure 6: Modified model ***M2*** [13].

2.3 Analysis of acoustic modes.

The simplest way to calculate acoustic modes of a vehicle cavity shown on Figure 1 is to use the approximation of a cavity by an equivalent rectangular enclosure having the same height H, width L and volume V. The resulting equivalent length A of a vehicle is then calculated as $A = V/HL$.

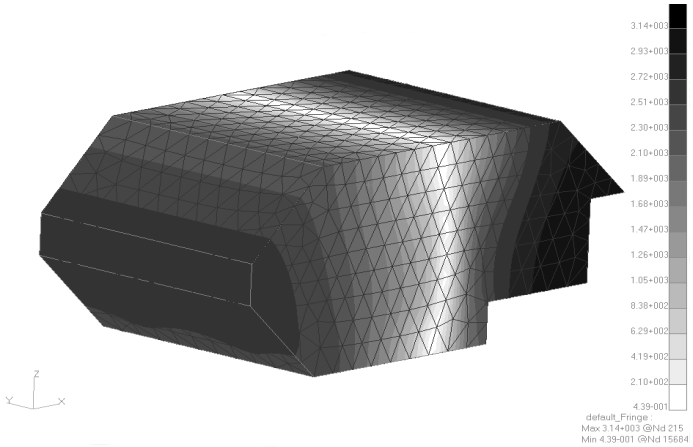

Figure 7: Finite element analysis of the lowest order acoustic mode of the irregular cavity [15]

This simple approximation gives remarkably good results at low frequencies. However, it fails for medium and higher frequencies, when the cavity shape becomes more important. In such cases finite element technique or other numerical methods can be used.

Figure 7 shows the results of finite element calculations of acoustic pressure for the lowest order acoustic mode of the irregular model cavity [15].

2.4 Calculation of structural-acoustic response

When all structural and acoustic modes have been determined the final step is to calculate the structural acoustic response of a model vehicle. This can be done e.g. by using analytical formulae discussed in the Section 2.1.

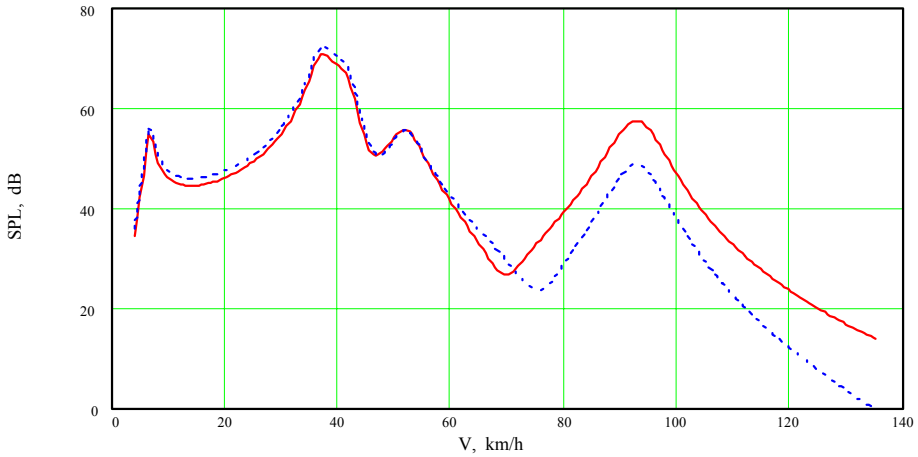

Figure 8: Calculated sound pressure level (SPL) of structure-borne noise in the vehicle compartment as a function of vehicle speed V on a sinusoidal road irregularity with the period d = 15 cm and height h = 1 cm for the locations of the front-left suspension: a) ls = 0.3 m (solid curve), b) ls = 0.45 m (dashed curve)

The results of typical calculations for a non-scaled simplified vehicle model are shown in Figure 8 as a function of vehicle speed. As one can see, at certain speeds corresponding to resonant frequencies of close structural and acoustic modes there are maxima of generated structure-borne interior noise.

An alternative way of calculating structural-acoustic response can be based on finite element analysis of coupled structural-acoustic modes and their excitation by a force applied to the structure [16].

3 Experiments with reduced-scale models

3.1 Measurements of structure-borne noise in QUASICAR

To carry out experimental investigations of basic mechanisms of structure-borne vehicle interior noise a reduced scale model, QUASICAR, has been designed and manufactured in Loughborough University (QUASICAR stands for QUArter Scale Interior Cavity Acoustic Rig). It is a ¼ scale representation of an average five-door saloon. The rig consists of a curved steel plate that is simply supported by two rigid side walls made of massive wooden panels (see Figure 9).

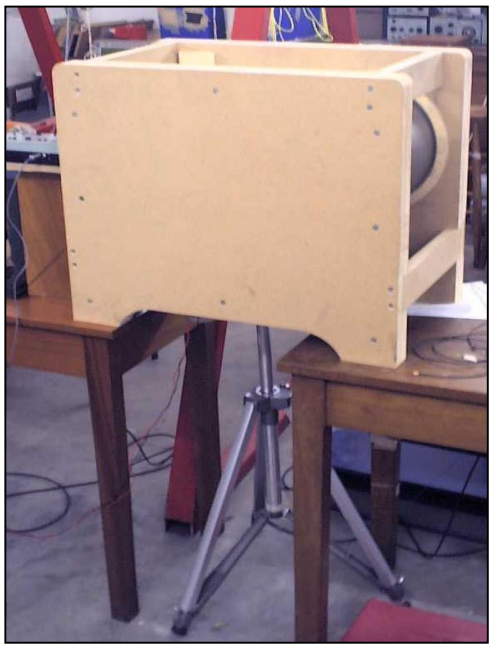

Figure 9: View of QUASICAR [9,10].

The principal component of the QUASICAR is the curved steel plate (see Figure 1) that simulates a flexible vehicle structure and forms an interior cavity. This plate was made of mild steel and was 1.2 mm thick. The side walls, made of massive wooden panels, were considered as absolutely rigid. The total length of the enclosed cavity, $a + 2R$, was 0.55m, the height, $H = 2R$, was 0.25m and the width, L, was 0.3m.

The electromagnetic shaker was applied to the bottom of the curved steel plate to generate structural vibrations associated with the effects of road irregularity transmitted via suspensions. The amplitudes of vibrations were measured by accelerometers. The location of the shaker was associated with the position of the front-right suspension of a vehicle. To measure sound pressure level (SPL) inside the cavity a sound

pressure level meter was used as well as microphones. The acoustic (air-borne) excitation was used to measure acoustic modes of the cavity and was provided by a miniature loudspeaker.

Figure 10 shows the results for structural and structural-acoustic responses for a shaker located in the position of the front-right suspension.

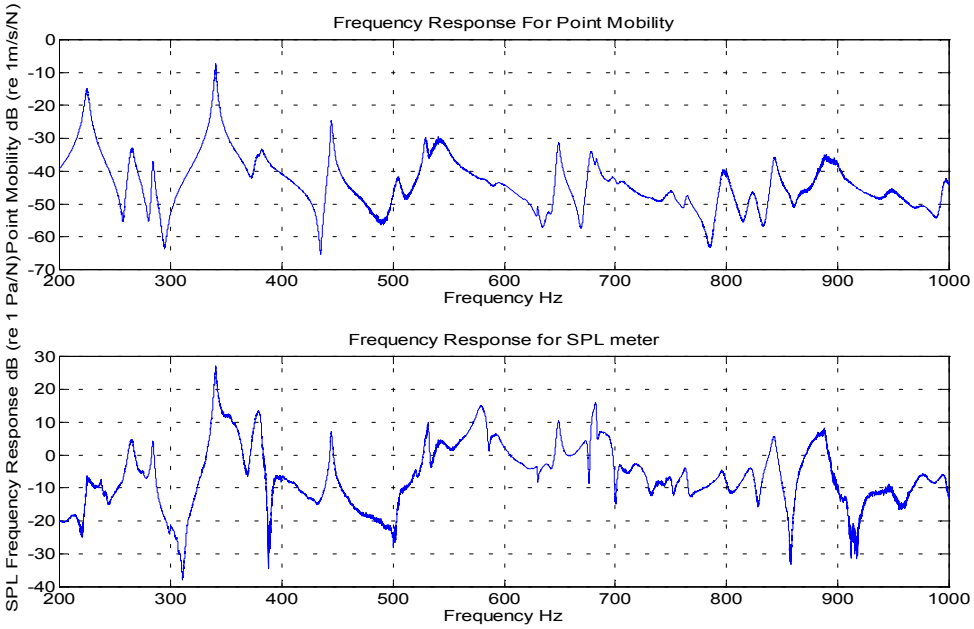

Figure 10: Structural and structural-acoustic responses of the QUASICAR. [9,10]

A comparison of the structural response of the plate (point mobility) and the corresponding structural acoustic response shows a good conceptual agreement with the theoretical model described in the Section 2.1. Indeed, as one can see from Figure 10, the principal resonance frequencies of the structure are being 'transmitted' into the structure-borne interior acoustic field, leading to high in-cavity noise levels. Comparison of the experimental results with the direct finite element calculations of structural-acoustic response [16] shows good quantitative agreement between theory and experiment.

3.2 Measurements of acoustic properties of some reduced-scale models.

To identify a permitted level of model simplification providing an acceptable agreement between its acoustic response and the response of a real vehicle three quarter-scale models of gradually increasing complexity have been used in the experiments [15]. The basic element of all three models was the rectangular wooden box with the dimensions 0.55 x 0.35 x 0.25m^3 (see Figure 11a). Then, to give a better representation of a car interior, extra sides made of wood of the same thickness (12 mm) were added to the corners of the model, resulting in the octagonal shaped cavity (Figure 11b). The final quarter-scale model represented the above-mentioned octagonal cavity with added seats made out of 50mm wooden blocks (Figure 11c). One of the sides making the octagonal cavity was taken out to give extra room in the model. On a later stage, felt material was added to the interior of all three cavities under investigation to study the absorption effect of trim which is always present in a real vehicle interior.

(*a*)

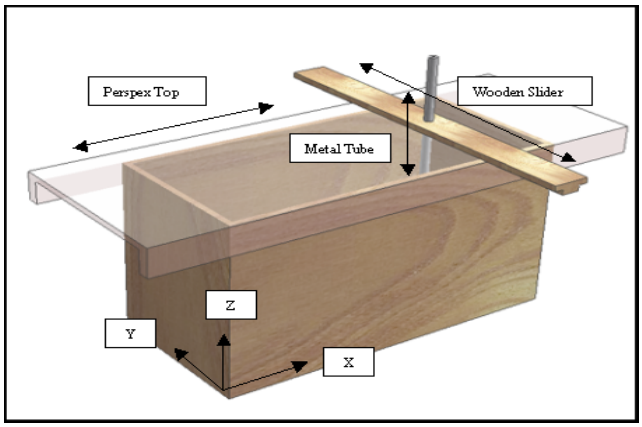

(*b*)

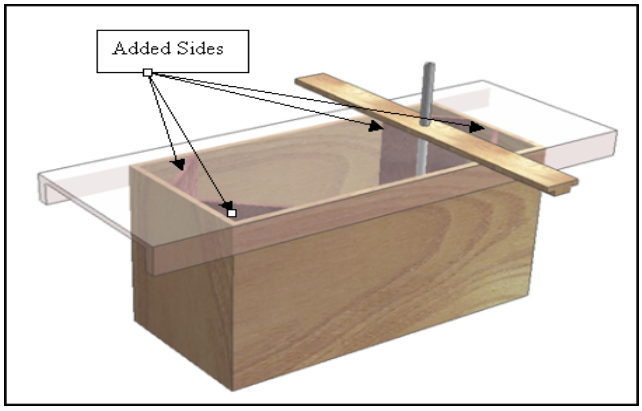

(*c*)

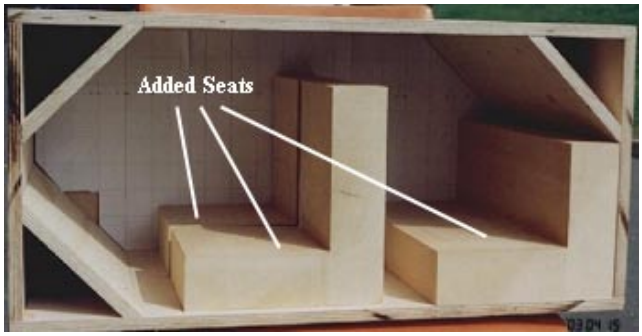

Figure 11: Diagrams of the rectangular (*a*) and octagonal (*b*) cavities, and a photograph of the irregular cavity with added seats (*c*) [15].

Measurements of sound pressure level and mode shapes were taken also in the interior of a real Ford Fiesta. The comparison of the measured frequency response of the irregular cavity (shown on Figure 11c) with added felt with the response of the Ford Fiesta is shown on Figure 12 (the measured resonant frequencies of the irregular cavity have been quartered to make the comparison possible). One can see that the curves behave in a very similar way. However, the measured SPL in the real vehicle is considerably lower, which is mainly due to the larger volume of the real vehicle compartment (by $4^3 = 64$ times, which corresponds to 36 dB). Since the volume of the enclosure is present in the denominator of the acoustic Green's function, the average theoretical SPL of a full-scale vehicle should be by around 36 dB lower. In reality, the sound absorbing effects of the felt in the model and of the trim in the real vehicle, that can not be scaled, might have caused the observed difference between the two curves being smaller than the above-mentioned 36 dB.

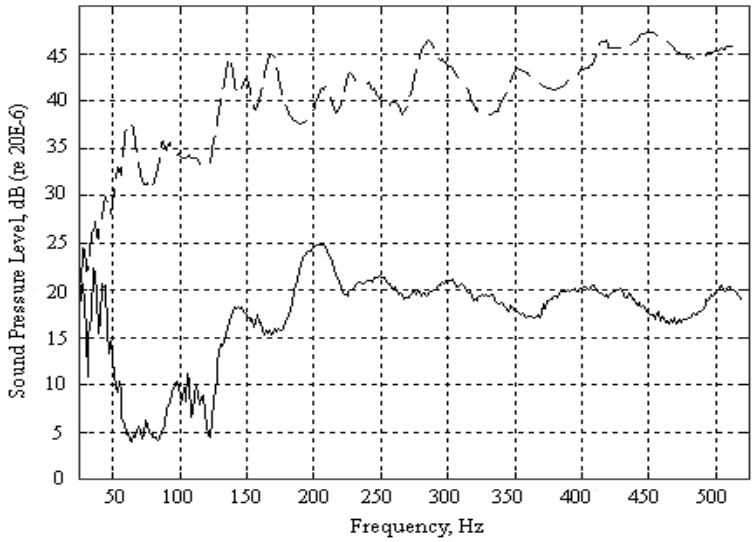

Figure 12. Frequency response of the Ford Fiesta compared with the response of the irregular cavity with added felt, solid and dashed curves respectively [15].

Further investigations of the effects of shape changes of vehicle interior cavity are required to understand their effects on frequency responses and modal shapes. The key practical issue here is to find a compromise between the minimum degree of complexity of a model and the required accuracy in description of frequency contents and noise levels in a real vehicle. It is expected that further development of techniques based on theoretical and experimental investigations of reduced-scale models will lead to the development of efficient analytical and experimental tools that could be suitable for prediction of vehicle interior noise on a design stage.

4 Conclusions

Research into vehicle interior noise using reduced-scale simplified models of road vehicles has demonstrated the ability of this technique to explain and predict structure-borne interior noise in real vehicles.

Although the models considered so far are overly simplified in comparison with real vehicle structures, they prove to be useful for basic understanding and explanation of main features of noise generation in road vehicles.

It is anticipated that introduction of more sophisticated but still manageable reduced-scale models reflecting the complexity of real vehicles will lead to the development of efficient analytical and experimental tools that could be suitable for prediction of vehicle interior noise on a design stage. The key practical issue here is to find a compromise between the minimum degree of complexity of a model and the required accuracy of description of frequency contents and noise levels in a vehicle.

References

[1] T. Priede, *Origins of automotive vehicle noise*, Journal of Sound and Vibration, Vol. 15, Academic Press (1971), pp. 61-73.

[2] S.K. Jha, *Characteristics and sources of noise and vibration and their control on motor cars*, Journal of Sound and Vibration, Vol. 47, Academic Press (1976), pp. 543-558.

[3] D.J. Nefske, J.A. Wolf, Jr. and L.J. Howell, *Structural-acoustic finite element analysis of the automobile passenger compartment: a review of current practice,* Journal of Sound and Vibration, Vol. 80, Academic Press (1982), pp. 247-266.

[4] S.H. Kim, J.M. Lee and M.H. Sung, *Structural-acoustic modal coupling analysis and application to noise reduction in a vehicle passenger compartment*, Journal of Sound and Vibration, Vol. 225, Academic Press (1999), pp. 989-999.

[5] T.C. Lim, *Automotive panel noise contribution modelling based on finite element and measured structural-acoustic spectra*, Applied Acoustics, Vol. 60, Elsevier (2000), pp. 505-519.

[6] V.V. Krylov, *Simplified analytical models for prediction of vehicle interior noise*, *Proceedings of the International Conference on Noise and Vibration Engineering (ISMA 2002)*, Leuven, Belgium, 16-18 September 2002, Ed. P. Sas, Vol. V, Leuven (2002), pp. 1973-1980.

[7] J.G. Cherng, G. Yin, R.B. Bonhard and M. French, *Characterisation and validation of acoustic cavities of automotive vehicles*, SPIE paper, Vol 1 (2002), pp 290-294.

[8] P. Chen and G. Ebbitt, *Noise absorption of automotive seats*, SAE paper, (1998), Ref: 980659.

[9] V.V. Krylov, S.J. Walsh and R.E.T.B. Winward, *Modelling of vehicle interior noise at reduced scale*, *Proceedings of EuroNoise 2003*, Naples, Italy, 19-21 May 2003, Naples (2003) (on CD).

[10] V.V.Krylov, S.J. Walsh and R.E.T.B. Winward, *Investigation of structural-acoustic coupling in a thin-walled reduced-scale model of a car*, *Proceedings of the International Conference on Thin-Walled Structures* (ICTWS-2004), Loughborough, UK, 22-24 June 2004, Ed. J. Loughlan, Institute of Physics, London (2004).

[11] M.C. Junger and D. Feit, *Sound, Structures and their Interaction*, Cambridge MA, MIT Press (1972).

[12] F. Fahy, *Sound and Structural Vibration*, London, Academic Press (1985).

[13] V.B. Georgiev, V.V. Krylov and R.E.T.B. Winward, *Finite element analysis of structural-acoustic interaction in simplified models of road vehicles*, Proceedings of the Institute of Acoustics, Vol. 26, Pt. 2, Institute of Acoustics (2004), pp. 25-36.

[14] V.V. Krylov and V.B. Georgiev, *Coupled-wave theory approach to understanding resonant vibrations of non-circular cylindrical shells*, Proceedings of the Institute of Acoustics, Vol.26, Pt. 2, Institute of Acoustics (2004), pp. 139-146.

[15] R. Gorman and V.V. Krylov, *Investigation of acoustic properties of vehicle compartments using reduced-scale simplified models*, Proceedings of the Institute of Acoustics, Vol.26, Pt. 2, Institute of Acoustics (2004), pp. 37-48.

[16] V.B. Georgiev, V.V. Krylov and R.E.T.B. Winward, *Finite element calculations of structural-acoustic modes of vehicle interior for simplified models of motorcars*, *Proceedings of InterNoise 2004*, Prague, Czech Republic, 22-25 August 2004 (on CD).